

Probing QCD Parameters with Top-Quark Data

Sebastian Naumann-Emme for the ATLAS and CMS Collaborations
DESY, Notkestraße 85, 22607 Hamburg, Germany

DOI: will be assigned

Results from inclusive and differential measurements of the production cross sections for top quarks in proton-proton collisions at center-of-mass energies of 7 and 8 TeV are compared to predictions at next-to-leading and next-to-next-to-leading order in perturbative Quantum Chromodynamics. From these studies, constraints on the top-quark mass, the strong coupling constant, and on parton distributions functions are determined.

1 Introduction

Quantum Chromodynamics (QCD) is the theory of the strong interaction between quarks and gluons. The only free parameters of the QCD Lagrangian are the quark masses and the strong coupling constant, α_S . The factorization theorem of QCD allows the calculation of cross sections, σ , to be split into hard-scattering matrix elements, $\hat{\sigma}$, on the one hand and parton distribution functions (PDFs) on the other. While $\hat{\sigma}$, describing the short-distance structure of a reaction, is process-dependent but perturbatively calculable, the PDFs, which account for the non-perturbative long-distance structure, are universal but have to be determined from experimental data.

The top quark is by far the heaviest of all quarks. Measurements of the top-quark mass, m_t , have been brought to an impressive precision at the Tevatron, $m_t = 173.20 \pm 0.87$ GeV [1], and at the Large Hadron Collider (LHC), $m_t = 173.20 \pm 0.95$ GeV [2]. However, exact relations between these results and theoretically well defined mass schemes have not yet been established.

The strong coupling constant has been measured in numerous processes and at different energies. The latest world average, which takes the mass of the Z boson as reference scale, is $\alpha_S(m_Z) = 0.1184 \pm 0.0007$ [3]. This average and its remarkable precision are driven by results obtained at relatively low energies, namely from hadronic decays of τ leptons and from lattice QCD. Cross sections for jet production at the LHC allow α_S to be probed even up to the TeV scale. However, the corresponding jet cross sections have typically been calculated only to next-to-leading order (NLO) QCD so far and they suffer from sizable uncertainties related to choice and variation of the renormalization and factorization scales, μ_R and μ_F , as well as from non-perturbative corrections.

PDF groups have released a large number of different PDF sets. For a given order in perturbation theory, the main differences between these PDF sets arise from the choice of the included data, the treatment of systematic uncertainties in the data and of correlations, the parametrization at the starting scale, the chosen heavy-quark scheme, and the values of the quark masses and of $\alpha_S(m_Z)$. At present, all PDF sets exhibit a significant uncertainty on the gluon density at medium-high parton momentum fractions, x . This uncertainty affects

predictions for Higgs-boson, top-quark, and jet production as well as many scenarios for new physics beyond the standard model.

In this article, constraints on PDFs, $\alpha_S(m_Z)$, and m_t from LHC top-quark data as well as their interplay are discussed. In general, the evolution of such QCD analyses is as follows: First, identify and potentially maximize the sensitivity of experimental data to the parameters of interest. Then, understand correlations, both between theory parameters and within the data. And, eventually, improve PDFs or determine other parameters by including the new data in QCD fits.

2 Top-Quark Pair Production

2.1 The Total Cross Section

At the LHC, top quarks are produced at relatively high rate, predominantly in pairs of quarks and anti-quarks ($t\bar{t}$) from gluon-gluon fusion. The calculation of the total $t\bar{t}$ cross section, $\sigma_{t\bar{t}}$, to next-to-next-to-leading order (NNLO) plus next-to-next-to-leading-log (NNLL) resummation has recently been completed [4]. The uncertainties related to higher orders, estimated via the variation of μ_R and μ_F , to the PDFs, to $\alpha_S(m_Z)$, and to m_t now amount to roughly 3% each. From the experimental point of view, $\sigma_{t\bar{t}}$ has been measured by the ATLAS and CMS Collaborations at proton-proton center-of-mass energies, \sqrt{s} , of 7 and 8 TeV, using the various $t\bar{t}$ decay channels. The most precise results have been obtained in the dilepton channel [5, 6], both of them yielding a total uncertainty on $\sigma_{t\bar{t}}$ below 5%.

The predicted $\sigma_{t\bar{t}}$ strongly depends on the assumed values of m_t and $\alpha_S(m_Z)$, but also the measured cross section can depend on them. Dependencies of the measured cross section arise from the acceptance corrections, which are derived using simulated $t\bar{t}$ events. Figure 1 compares CMS' most precise single measurement of $\sigma_{t\bar{t}}$ [5], which was obtained at $\sqrt{s} = 7$ TeV, to the NNLO+NNLL prediction with five different NNLO PDF sets. These PDF sets are provided for a series of $\alpha_S(m_Z)$ values, which allows the full correlation between the choice of $\alpha_S(m_Z)$ and the parton densities to be preserved. Relatively small differences are found between four of the five PDF sets, namely between CT10, HERAPDF1.5, MSTW2008, and NNPDF2.3. ABM11, by contrast, does not only have a smaller default value of $\alpha_S(m_Z)$ but also a smaller gluon density, which results in a lower $\sigma_{t\bar{t}}$ prediction compared to the other PDF sets at any given $\alpha_S(m_Z)$ value. While the measured $\sigma_{t\bar{t}}$ has a sizable m_t dependence, only a minor dependence on $\alpha_S(m_Z)$ was found.

CMS used this comparison between measured and predicted $\sigma_{t\bar{t}}$ for extractions of m_t and $\alpha_S(m_Z)$ [7]. The NNLO+NNLL prediction was taken as a Bayesian prior to the cross-section measurement, which enabled the construction of marginalized posteriors in m_t and $\alpha_S(m_Z)$. The measured cross section was parametrized using a Gaussian probability function along $\sigma_{t\bar{t}}$. The PDF uncertainty on the predicted $\sigma_{t\bar{t}}$ was also assumed to be Gaussian and convoluted with a step function that yields equal probabilities for all $\sigma_{t\bar{t}}$ values covered by the μ_R and μ_F variations and vanishes elsewhere. No big changes were found when trying different parametrizations for the scale uncertainty. The marginalized posteriors were then obtained by integrating over $\sigma_{t\bar{t}}$. For given values of $\alpha_S(m_Z)$ or m_t , these posteriors yield the most probable m_t and $\alpha_S(m_Z)$ values, respectively, together with Bayesian confidence intervals that account for the uncertainty on the measured cross section and the PDF and scale uncertainties on the predicted cross section. Additionally, the following uncertainties were taken into account:

- An uncertainty of 0.65% on the LHC beam energy (E_{LHC}) [8], translating into 46 GeV on the nominal \sqrt{s} value of 7 TeV.
- For the m_t determination, the uncertainty of 0.0007 on the $\alpha_S(m_Z)$ world average, which was used as constraint.
- For the m_t determination, an uncertainty of 1 GeV on the equality of top-quark pole mass and the top-quark mass in the Monte Carlo simulation (m_t^{MC}) [9], since the simulation was employed for the acceptance corrections in the $\sigma_{t\bar{t}}$ measurement.
- For the $\alpha_S(m_Z)$ determination, an uncertainty of 1.4 GeV on the Tevatron average for m_t , which was used as constraint. This variation accounts for both the 0.9 GeV uncertainty of the Tevatron average itself and the 1 GeV uncertainty in relating m_t^{MC} , employed also to calibrate these direct mass measurements, to the top-quark pole mass.

Using NNPDF2.3, the results are

$$\begin{aligned}
m_t &= 176.7_{-2.8}^{+3.1}(\text{exp.})_{-1.3}^{+1.5}(\text{PDF})_{-0.9}^{+0.9}(\text{scale})_{-0.7}^{+0.7}(\alpha_S)_{-0.9}^{+0.9}(E_{\text{LHC}})_{-0.4}^{+0.5}(m_t^{\text{MC}}) \text{ GeV} \\
&= 176.7_{-3.4}^{+3.8} \text{ GeV}
\end{aligned}$$

and, alternatively,

$$\begin{aligned}
\alpha_S(m_Z) &= 0.1151_{-0.0025}^{+0.0025}(\text{exp.})_{-0.0011}^{+0.0013}(\text{PDF})_{-0.0008}^{+0.0009}(\text{scale})_{-0.0013}^{+0.0013}(m_t)_{-0.0008}^{+0.0008}(E_{\text{LHC}}) \\
&= 0.1151_{-0.0032}^{+0.0033}.
\end{aligned}$$

The results with all five PDF sets are shown in Figure 2. These are the first extractions of the top-quark pole mass at full NNLO QCD, of $\alpha_S(m_Z)$ from top-quark data, and of $\alpha_S(m_Z)$ at full NNLO QCD from a hadron collider. There are only small differences between the result obtained with CT10, HERAPDF1.5, MSTW2008, and NNPDF2.3, while the smaller gluon density of ABM11 requires either a lower m_t or a higher $\alpha_S(m_Z)$ value to reproduce the $\sigma_{t\bar{t}}$ measured by CMS. Using ABM11 with its default $\alpha_S(m_Z)$ of 0.1134 ± 0.0011 would yield $m_t = 166.3_{-3.1}^{+3.3}$ GeV, which is significantly lower than the results from direct m_t measurements and than the results obtained via $\sigma_{t\bar{t}}$ when using the other PDF sets.

First studies illustrating the impact of the total $\sigma_{t\bar{t}}$ as measured at LHC and Tevatron in particular on the gluon PDF have been released by different authors [10, 11, 12]. However, more work is needed to accurately incorporate all systematic uncertainties and correlations, both between the PDFs, α_S , and m_t and among the experimental data, as well as the experimental m_t dependencies. Ratios of the $t\bar{t}$ cross section measured at different center-of-mass energies (8 to 7 TeV; later: 14 to 8 TeV) also have promising prospects for PDF fits, since the PDF uncertainties on the predicted ratios are significantly larger than the combined μ_R , μ_F , α_S , and m_t uncertainties [11], but such cross-section ratios require a thorough understanding of the correlations between the systematic uncertainties on the measured $\sigma_{t\bar{t}}$ at the different center-of-mass energies.

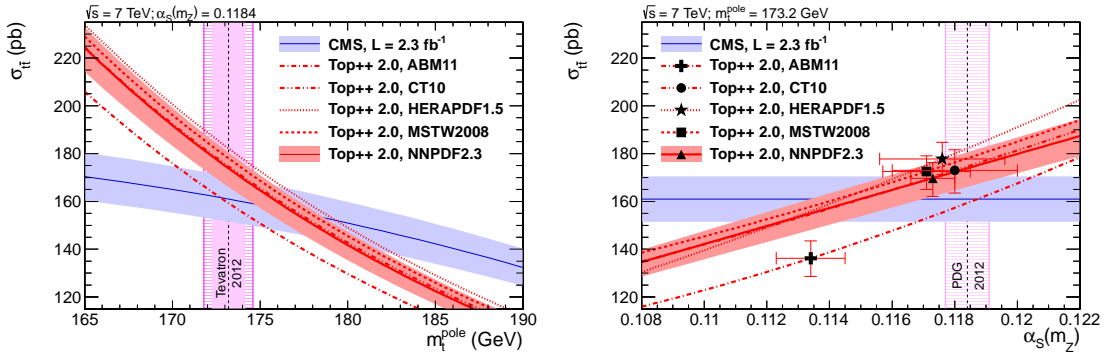


Figure 1: Predicted $t\bar{t}$ cross section at NNLO+NNLL, as a function of the top-quark mass (left) and of the strong coupling constant (right), using five different NNLO PDF sets, compared to the cross section measured by CMS [7].

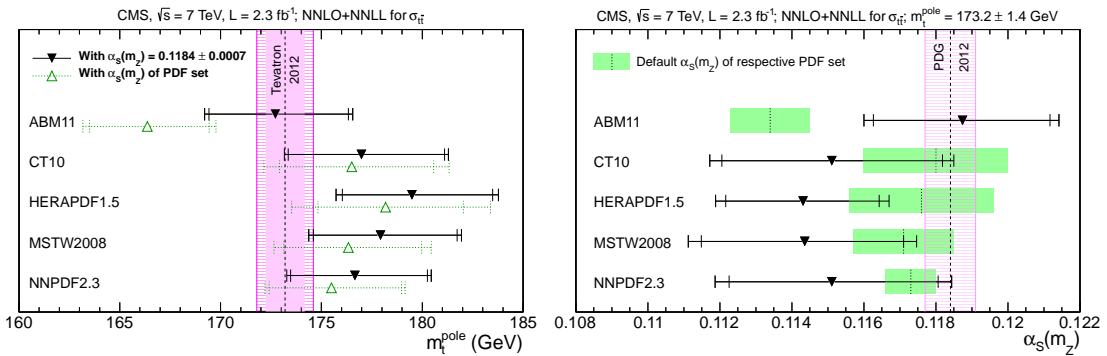


Figure 2: Results obtained for the top-quark mass (left) and for the strong coupling constant (right) by comparing the measured $t\bar{t}$ cross section from CMS to the prediction at NNLO+NNLL using five different NNLO PDF sets [7].

2.2 Differential Cross Sections

ATLAS and CMS have measured a variety of (normalized) differential cross sections for $t\bar{t}$ production [13, 14, 15, 16, 17]. These results, discussed in more detail in [18], can be compared to predictions at NLO or, in some cases (namely the distributions as a function of the transverse momentum and the rapidity of the top-quarks as well as the invariant mass of the $t\bar{t}$ system), to calculations at approximate NNLO.

In general, kinematic regions in which the PDF uncertainty on the predicted cross section is larger than other modeling uncertainties are considered to have the largest potential to improve the accuracy of future PDF fits. The ATLAS Collaboration compared differential $t\bar{t}$ cross sections at $\sqrt{s} = 7$ TeV to predictions at NLO QCD with different NLO PDF sets [19, 17]. The best PDF sensitivity was found in the rapidity and the invariant mass of $t\bar{t}$ system, $y_{t\bar{t}}$ and $m_{t\bar{t}}$. The size of the corresponding theory uncertainties are illustrated in Figure 3. Both $y_{t\bar{t}}$ and $m_{t\bar{t}}$ are directly correlated with the momenta of the incoming partons. Large rapidities require one incoming parton with high x , the other one with small x . Large $m_{t\bar{t}}$ values also probe the high- x regime. However, it has to be kept in mind that electroweak corrections to differential $t\bar{t}$ cross section are known to be non-negligible, in particular for high transverse momenta and invariant masses but also for the shape of the $y_{t\bar{t}}$ distribution (as discussed, for example, in [20]), and that these corrections are typically not yet included in these comparisons.

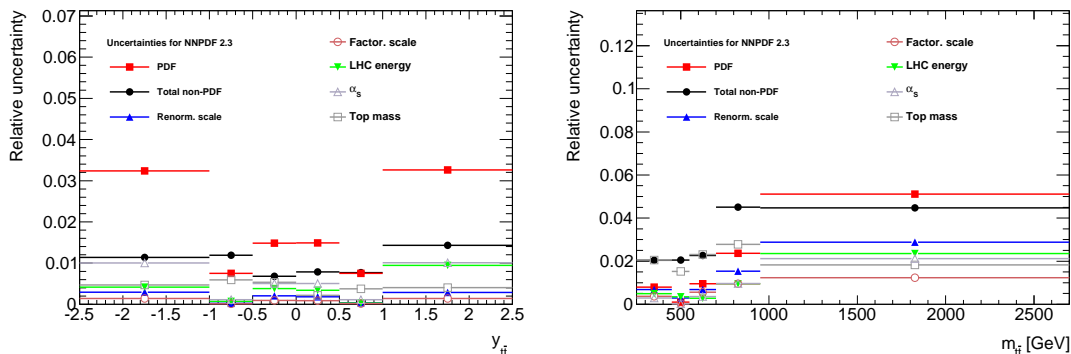


Figure 3: Relative uncertainties on the NLO prediction with NNPDF2.3 for the normalized $t\bar{t}$ cross section as a function of the rapidity (left) and the invariant mass (right) of the $t\bar{t}$ system [19].

Using the first 2.1 fb⁻¹ of data at $\sqrt{s} = 7$ TeV, ATLAS quantified the compatibility between measured differential cross sections in the lepton+jets channel and the corresponding NLO predictions with five different NLO PDF sets (ABM11, CT10, HERAPDF1.5, MSTW2008, NNPDF2.3), taking into account all experimental and theoretical uncertainties as well as bin-to-bin correlation for the data [19]. The best separation strength was found for $y_{t\bar{t}}$, where the χ^2 probabilities range from 21% for CT10 to 83% for NNPDF2.3.

Recently, the ATLAS Collaboration released updated results for differential $t\bar{t}$ cross sections [17], now using the full dataset at 7 TeV, corresponding to 4.6 fb⁻¹. The compatibility between data and NLO prediction is shown in Figure 4 for $y_{t\bar{t}}$, $m_{t\bar{t}}$, and the transverse momentum of the top quarks, $p_{T,t}$. In all three cases, a significant tension in shape between the predictions with the various PDF sets can be seen. As before, the level of agreement between

data and prediction appears to be better with MSTW2008 than with CT10 and better with NNPDF2.3 compared to MSTW2008. However, the new data seems to prefer the prediction with HERAPDF1.5. Again, electroweak corrections are not yet included here but could yield a non-negligible contribution.

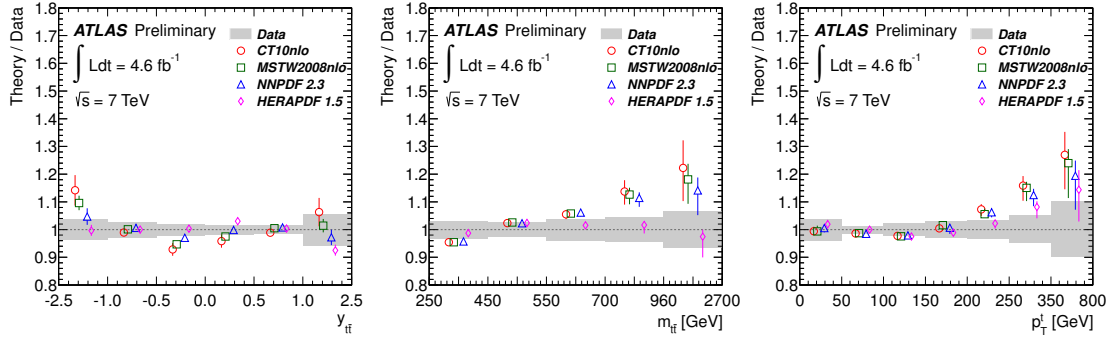


Figure 4: Ratios of the NLO predictions with four different NLO PDF sets to the measured normalized $t\bar{t}$ cross section as a function of rapidity (left) and invariant mass (center) of the $t\bar{t}$ system as well as the transverse momentum of the top quarks (right) [17].

3 Production of Single Top Quarks

The production of single top quarks occurs via weak, charged-current interactions. At the LHC, the dominant process is the t-channel exchange of a virtual W boson between a light quark from one of the colliding protons and a bottom quark from the other proton. Since the up-quark density in protons is about twice as high as the down-quark density, the cross section for the production of single top quarks is about twice as high as the cross section for single anti-top quarks. Precise measurements of the ratio $R_t = \frac{\sigma_t}{\sigma_{\bar{t}}}$ can provide a handle on the ratio of the u/d densities in the proton. They probe the kinematic regime $0.02 \lesssim x \lesssim 0.5$ and are thus complementary to measurements via the charge asymmetry in W-boson production, which probe $0.001 \lesssim x \lesssim 0.1$ at the LHC and $0.005 \lesssim x \lesssim 0.3$ at the Tevatron.

The ratio R_t has been measured by ATLAS [21] and CMS [22] at $\sqrt{s} = 7$ TeV and 8 TeV, respectively, to be:

$$\begin{aligned} R_t(7 \text{ TeV}) &= 1.81 \pm 0.10 \text{ (stat.) } {}^{+0.21}_{-0.20} \text{ (syst.)} = 1.81^{+0.23}_{-0.22}, \quad \text{and} \\ R_t(8 \text{ TeV}) &= 1.76 \pm 0.15 \text{ (stat.) } \pm 0.22 \text{ (syst.)} = 1.76 \pm 0.27. \end{aligned}$$

In both cases, the sign of the top-quark charge was inferred from the reconstructed charge of the final-state lepton that had been associated to the top-quark decay. The observed R_t are compatible with the predictions at NLO QCD. This is shown in Figure 5 using predictions with various PDF sets. The spread of the predictions with different PDF sets is approximately of the same size as the uncertainty on the predictions. Apart from the light-quark PDFs and the renormalization and factorization scales, the predicted cross sections for single top-quark production depend also on the choice of the heavy-flavor scheme (fixed-flavor schemes with four

or five active flavors versus variable flavor schemes), the bottom-quark density in the proton, and the bottom-quark mass. However, the uncertainty on the measured R_t is currently still roughly more than twice as large as the total uncertainty on the prediction.

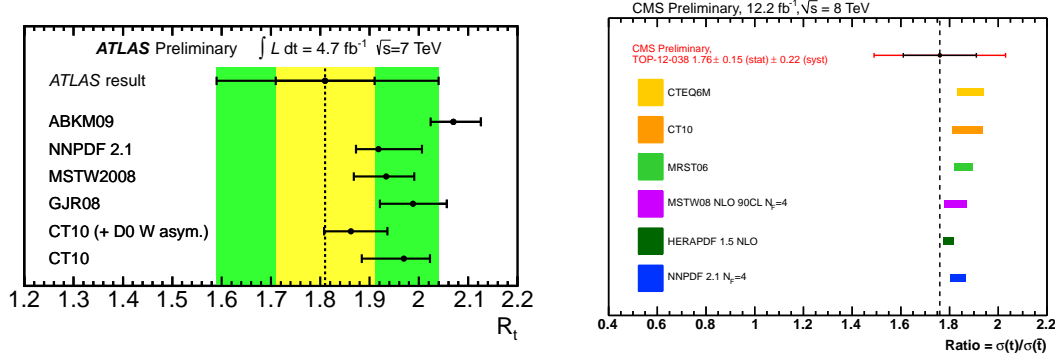


Figure 5: Comparisons between the ratio of the production cross sections for single top quarks and single anti-top quarks, measured by ATLAS at $\sqrt{s} = 7 \text{ TeV}$ (left) [21] and by CMS at 8 TeV (right) [22], and the NLO prediction with various PDF sets.

4 Conclusions

The large samples of top-quark data that are being collected at the LHC enable new and ever more precise QCD analyses.

The precisely measured total cross section for $t\bar{t}$ production together with the prediction at NNLO+NNLL QCD allows for extractions of the top-quark pole mass that are significantly more precise than previous determinations of the top-quark mass from cross sections. Alternatively, when constraining m_t to the average of previous measurements, the $t\bar{t}$ cross section enables the first $\alpha_S(m_Z)$ determination at NNLO QCD at a hadron collider. The precision is competitive with other $\alpha_S(m_Z)$ measurements. Furthermore, the inclusive $t\bar{t}$ cross section is currently the only process that directly allows the high- x gluon PDF to be probed at full NNLO QCD. An improved precision on the gluon PDF is crucial not only for future top-quark analyses but also many Higgs-boson analyses and new-physics searches. Differential $t\bar{t}$ cross sections are starting to allow for even more explicit PDF discrimination. The most sensitive distributions are the differential cross sections as a function of the rapidity and the invariant mass of the $t\bar{t}$ system. In any of these QCD analyses using $t\bar{t}$ cross sections, it is imperative to consider the full correlations between m_t , α_S , and the gluon PDF as well as the correlations within the experimental data.

A handle on the ratio of the u -quark to d -quark PDFs can eventually be obtained from more precise measurements of the charge ratio in t -channel production of single top quarks.

References

- [1] The Tevatron Electroweak Working Group and CDF and D0 Collaborations, arXiv:1305.3929 [hep-ex].
- [2] The ATLAS and CMS Collaborations, ATLAS-CONF-2013-102, CMS-PAS-TOP-13-005.
- [3] J. Beringer *et al.* [Particle Data Group Collaboration], Phys. Rev. D **86** (2012) 010001.
- [4] M. Czakon, P. Fiedler and A. Mitov, Phys. Rev. Lett. **110** (2013) 252004 [arXiv:1303.6254 [hep-ph]].
- [5] S. Chatrchyan *et al.* [CMS Collaboration], JHEP **1211** (2012) 067 [arXiv:1208.2671 [hep-ex]].
- [6] The ATLAS collaboration, ATLAS-CONF-2013-097.
- [7] S. Chatrchyan *et al.* [CMS Collaboration], arXiv:1307.1907 [hep-ex].
- [8] J. Wenninger, CERN-ATS-2013-040.
- [9] A. Buckley *et al.*, Phys. Rept. **504** (2011) 145 [arXiv:1101.2599 [hep-ph]].
- [10] M. Beneke *et al.*, JHEP **1207** (2012) 194 [arXiv:1206.2454 [hep-ph]].
- [11] M. Czakon, M. L. Mangano, A. Mitov and J. Rojo, JHEP **1307** (2013) 167 [arXiv:1303.7215 [hep-ph]].
- [12] S. Alekhin, J. Blümlein and S. Moch, arXiv:1310.3059 [hep-ph].
- [13] G. Aad *et al.* [ATLAS Collaboration], Eur. Phys. J. C **73** (2013) 2261 [arXiv:1207.5644 [hep-ex]].
- [14] S. Chatrchyan *et al.* [CMS Collaboration], Eur. Phys. J. C **73** (2013) 2339 [arXiv:1211.2220 [hep-ex]].
- [15] The CMS Collaboration, CMS-PAS-TOP-12-027.
- [16] The CMS Collaboration, CMS-PAS-TOP-12-028.
- [17] The ATLAS Collaboration, ATLAS-CONF-2013-099.
- [18] M. Aldaya, these proceedings.
- [19] The ATLAS Collaboration, ATLAS-PHYS-PUB-2013-008.
- [20] J. H. Kühn, A. Scharf and P. Uwer, arXiv:1305.5773 [hep-ph].
- [21] The ATLAS Collaboration, ATLAS-CONF-2012-056.
- [22] The CMS Collaboration, CMS-PAS-TOP-12-038.